ELSEVIER

Catalysis Today 78 (2003) 291–301

CATALYSIS TODAY

www.elsevier.com/locate/cattod

The beneficial effect of cobalt on VPO catalysts

L. Cornaglia [a],*, S. Irusta [a], E.A. Lombardo [a], M.C. Durupty [b], J.C. Volta [b]

[a] *Instituto de Investigaciones en Catálisis y Petroquímica, INCAPE (FIQ, UNL-CONICET), Santiago del Estero 2829, 3000 Santa Fe, Argentina*

[b] *Institut de Recherches sur la Catalyse, CNRS, 2 Av. A. Einstein, 69626 Villeurbanne Cedex, France*

Abstract

The addition of Co to VPO formulations improves the yield of *n*-butane to maleic anhydride. In this work, different modes of impregnation and two different organic cobalt salts were used. The equilibrated catalysts were characterized using XRD, ^{31}P SEM NMR, FT-IR and acetonitrile adsorption to evaluate Lewis acidity.

The best catalyst was obtained using Co acetyl acetonate for impregnation of the $VOHPO_4 \cdot 0.5H_2O$ precursor. This catalyst after equilibration had an optimum concentration of very strong Lewis acid sites, very low concentration of isolated V(V) centers, and no V(V) phases.

Keywords: Cobalt promoter; VPO catalysts; Acidity; Maleic anhydride; *n*-Butane oxidation

1. Introduction

Vanadyl pyrophosphate exhibits a unique ability to activate and selectively oxidize *n*-butane to maleic anhydride. It is generally agreed upon that the best catalyst precursor is $VOHPO_4 \cdot 0.5H_2O$. The hemihydrate precursors are usually obtained by reduction of pentavalent vanadium compounds with organic reductive agents, such as a mixture of isobutanol and benzyl alcohol [1]. In other cases, only the less reductive isobutanol is employed [2]. The precursor is converted to $(VO)_2P_2O_7$ [1] during activation. Besides, several $VOPO_4$ phases present in low proportion have been claimed as necessary for the catalytic act [2].

A variety of cations have been added to vanadium phosphorus catalysts to improve activity and selectivity. The role of promoters added to the VPO formulations is still unresolved and controversial. Several papers [3–9] refer to the effect of cobalt used as a promoter. Takita et al. [5] sustained that the additives were incorporated into the crystal lattice of vanadyl pyrophosphate. Other authors [4,6,7] studied the influence of cobalt addition on the composition of the $(VO)_2P_2O_7$ catalyst. The presence of cobalt enhanced surface phosphorus enrichment, which modified the surface acidity. Zazhigalov et al. [7] proposed that cobalt stabilize the catalyst performance by forming cobalt phosphate, which improves its catalytic properties.

The two groups that participate in this work have published several papers concerning the role of cobalt in VPO catalysts. However, their respective views on this matter are not strictly coincidental. Besides, different preparation methods and activation strategies were used to obtain the catalysts.

Volta and coworkers [10] compared the catalytic performances and microstructures of VPO materials doped with varying amounts of Co. The Co-doped VPO catalysts were prepared from the reaction of

---

* Corresponding author. Fax: +54-342-453-6861.
E-mail address: nfisico@fiqus.unl.edu.ar (L. Cornaglia).

0920-5861/02/$ – see front matter © 2002 Elsevier Science B.V. All rights reserved.
PII: S0920-5861(02)00315-2

V_2O_5 and H_3PO_4 or $VOPO_4{\cdot}2H_2O$ with isobutanol. The Co addition acts as a structural promoter. The smallest amounts of dopant produced the most beneficial effect. They also used in situ laser Raman spectroscopy [11] to study the evolution of the catalyst structure for materials derived from Co-$VOHPO_4{\cdot}0.5H_2O$ formed by the reaction with isobutanol. They found that the incorporation of Co can modify the V(V)/V(IV) balance during the activation period and can therefore change the catalytic performance in the steady state. By NMR techniques, they observed that the presence of the Co dopant inhibits the transformation of the precursor and stabilizes an amorphous vanadium phosphate.

Lombardo and coworkers [9,12] studied impregnated Co-VPO catalysts obtained with different cobalt salts and impregnation procedures. The hemihydrate precursor was prepared employing a mixture of isobutanol and benzyl alcohol. After 700 h on stream, the only phase detected in all cases was vanadyl pyrophosphate. Co acetyl acetonate allowed them to change the cobalt dispersion on the surface, and led to a more selective high loading catalyst. They studied the surface acidity of cobalt-impregnated solids using acetonitrile, and found a non-linear correlation between the concentration of very strong Lewis acid sites and maleic anhydride selectivity.

Accordingly, we exchanged samples and information in order to clarify the role of cobalt in connection with the co-existence of other VPO phases, the appearance of highly dispersed V(V) centers and the development of Lewis acidity. Co-impregnated equilibrated catalysts were characterized employing ^{31}P MAS NMR and SEM NMR techniques, XRD, XPS, and acetonitrile adsorption monitored by FT-IR.

2. Experimental

2.1. Catalyst preparation

The precursor was obtained by reduction of 5 g of V_2O_5 with 30 ml of isobutanol and 20 ml of benzyl alcohol under reflux for 3 h. Then orthophosphoric acid (100%) was added in the desired amount and the solution refluxed for another 2 h. After completion of the reaction, the solid phase was recovered by filtration and dried in air at 390 K overnight.

2.1.1. Promoted catalyst

The impregnation was carried out using either cobalt acetate or acetyl acetonate and following two procedures:

(a) The impregnation method: The salt, acetate (VPCo*x*-Ia) or acetyl acetonate of Co (VPCo*x*-Iaa, where *x* represents wt.% of Co), was dissolved in 30 ml of isobutanol. The previously prepared precursor was added to this solution and the suspension was heated to 330 K with continuous stirring. The solvent was evaporated and the wet solid dried at 390 K. The final Co content of all of the preparations was determined by atomic absorption.

(b) The high temperature impregnation method: Cobalt acetyl acetonate was used in this case (VPCo*x*-HTI). The salt was dissolved in a mixture of 30 ml of isobutanol and 20 ml of benzyl alcohol, the precursor was added and refluxed overnight. The reflux temperature was 393 K. The precipitate was then filtered and dried in air at 390 K.

2.2. Catalyst activation and testing

The promoted catalyst precursors and unpromoted VPO were activated in a fixed-bed microreactor. Typically, about 1 g of catalyst (screened 170/250 μm range Tyler 60/80 mesh) was loaded in the reactor and covered with a layer of quartz wool.

The quartz reactor was 60 cm long and 1.0 cm i.d. at the catalyst bed section. It was mounted vertically in a tubular furnace. A programmable temperature controller was used to assure reproducibility of heating strategies. Mass flow controllers were used to feed the reactants in the right proportion. An on-line gas chromatograph equipped with an FID detector was used to analyze both the reactant and product streams. Separation of C_4H_{10} and maleic anhydride was accomplished with a 2 ft 1/8 column packed with SS Chromosorb WAW AT-1200 + 1% H_3PO_4 80/100.

The activation of the catalyst was performed by heating from ambient temperature to 603 K while flowing a mixture of 0.75% *n*-butane in air, with a gas hourly space velocity (GHSV) of 900 h^{-1}. The temperature was kept constant at 603 K for 3 h. Those catalysts, which only underwent this treatment, are here called non-equilibrated catalysts. Then, the *n*-butane concentration was increased to 1.5% while still maintaining the GHSV at 900 h^{-1}. The temperature was raised until either 80% conversion or the maximum allowable temperature of 703 K was reached. Then, the GHSV was raised to 2500 h^{-1} and the temperature was slowly increased with the limitation that conversion never exceeded 80%. The catalytic data reported here were measured over solids that did not show any change in activity and selectivity after at least 500 h on stream. At this point, when the reaction temperature was randomly varied up and down, reproducible values of activities and selectivities were obtained. These solids are called equilibrated catalysts.

2.3. *Catalyst characterization*

2.3.1. *XRD*

The measurements were made with a Shimadzu XD-D1 X-ray diffractometer, using nickel-filtered Cu Kα radiation with a scanning rate of 1°/min.

2.3.2. *IR spectroscopy*

The IR spectra were obtained using a Shimadzu FT-IR 8101M spectrometer with a spectral resolution of 4 cm^{-1}. The solid samples were prepared in the form of pressed wafers (ca. 2 wt.% sample in KBr). The IR spectra of precursors were obtained using fluorolube as a diluting agent in order to explore the high wave number region.

The samples for the adsorption experiments were prepared by compressing the used catalysts at 9 t/cm^2 in order to obtain a self-supporting wafer (50 mg, 1 cm diameter). They were mounted on a transportable IR cell with CaF_2 windows and external oven. The pretreatment was performed in a high vacuum system. The sample was first outgassed at 723 K for 12 h in a dynamic vacuum of 7×10^{-4} Pa. After cooling to room temperature a spectrum of the catalyst wafer was taken. No bands were observed in the 1600 cm^{-1} region; this is indicative that molecular water was eliminated. After that, 4.8×10^4 Pa of acetonitrile were admitted into the cell, left in contact with the solid for 10 min, and then a spectrum was recorded. No changes were observed in the 1600 cm^{-1} region, therefore no water was introduced during acetonitrile adsorption. Spectra were also recorded after evacuation of the cell for 10 min at 298, 353 and 423 K.

2.3.3. *XPS*

The XPS measurements were carried out using an ESCA750 Shimadzu electron spectrometer. Non-monochromatic Al Kα X-ray radiation was used. The anode was operated at 8 kV and 30 mA and the pressure in the analysis chamber was about 2×10^{-6} Pa. The data were collected using an ESCAPAC 760 computer interfaced to the spectrometer and analyzed with the Googly software developed at the University of Pittsburgh.

The binding energies (BEs) were referred to the C 1s signal (284.6 eV). Curve fitting was performed using a Levenberg–Marquardt NLLSCF routine. The background contribution was taken into account by assuming an integral type background which was included in the basic shape of each peak. Account has been taken of the presence of $K\alpha_3$ and $K\alpha_4$ spectral lines of the large O 1s signal. These satellite peaks are 9.6 and 11.6 eV downshifted from the O 1s main peak and overlap the V $2p_{1/2}$ signal. Since the resolution of the V $2p_{1/2}$ is poorer than that of the V $2p_{3/2}$ level, we preferably used the latter BEs and widths for comparison with literature data. The V 2p and Co 2p doublets were fitted using a Voigt function with 20% Lorentzian character and $2p_{1/2}/2p_{3/2}$ intensity ratio = 0.5. Additional data for the curve fitting of the V 2p doublets include spin–orbit separation = 7.2 eV.

The surface P/V and Co/V atomic ratios were calculated using the areas under the Co $2p_{3/2}$, P 2p and V $2p_{3/2}$ peaks, the Scotfield photoionization cross sections, the mean free paths of the electrons and the instrumental function which was given by the ESCA manufacturer.

2.3.4. *NMR spectroscopy*

The ^{31}P NMR spectra were recorded with a BRUCKER DSX400 spectrometer, at 161.9 MHz, equipped with a standard 4 mm probe head. The ^{31}P spin echo mapping (SEM) spectra were obtained with a sweep width of 2 MHz, $t = 20$ ms and 90° pulse length of 1.5 ms.

3. Results

Fig. 1A and B show the catalytic behavior of the four formulations prepared for this study. The catalyst impregnated with cobalt acetyl acetonate (VPCo4-Iaa)

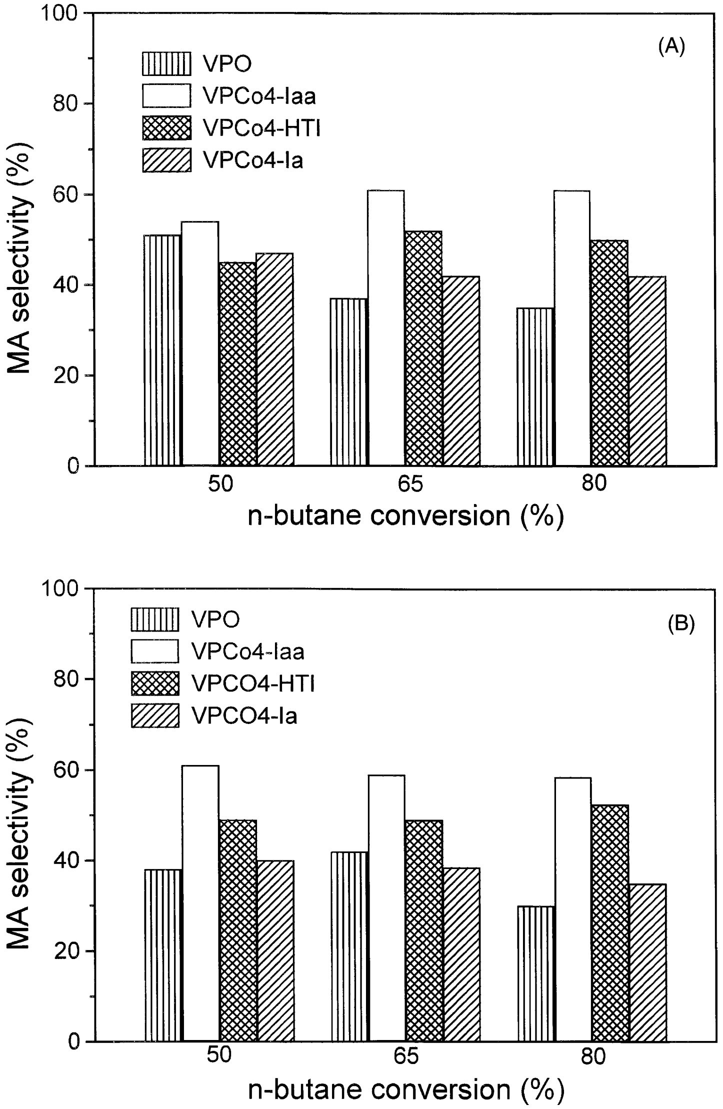

Fig. 1. Catalytic behavior of promoted and unpromoted catalysts. Reaction conditions: 1.5% *n*-butane/air. (A) GHSV $= 2500\,h^{-1}$; (B) GHSV $= 900\,h^{-1}$.

exhibits the highest selectivity to maleic anhydride. This applies to all the conversion range explored and at both space velocities (900 and $2500\,h^{-1}$). At $2500\,h^{-1}$ (Fig. 1A) the selectivities of all the solids are quite similar at 50% conversion. However, at higher conversions the beneficial effect of cobalt is evidenced. At lower space velocity ($900\,h^{-1}$) the solid impregnated with cobalt acetate does not differ much from the unpromoted VPO (Fig. 1B). In any case, those formulations prepared with the cobalt acetyl acetonate (VPCo4-Iaa and VPCo4-HTI) are both superior to the other two formulations (Fig. 1A and B).

XRD only reveals the presence of V(V) phases in the case of the acetate derived solid. Fig. 2 shows the diffraction patterns of both the acetate and one of the acetyl acetonate formulations. The former exhibits a reflection at $2\theta = 18.1^\circ$ which can be assigned to the presence of a small proportion of γ-$VOPO_4$ [2].

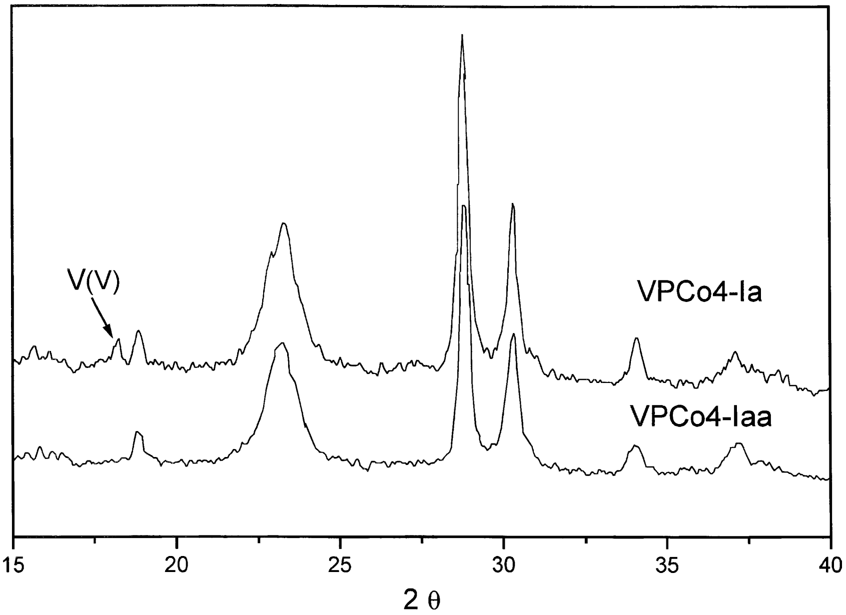

Fig. 2. XRD patterns of VPCo4-Ia and VPCo4-Iaa.

The ^{31}P SEM NMR spin echo mapping spectra (Fig. 3) show two major signals in the 2000–3500 ppm range [$(VO)_2P_2O_7$] and near 0 ppm (V(V) species and $VOPO_4$ phases). ^{31}P NMR by spin echo mapping gives information about the different oxidation states of vanadium surrounding the P atoms in $(VO)_2P_2O_7$ [13]. When cooling $(VO)_2P_2O_7$ at −123 °C, the large signal at 2000–3500 ppm has been observed to be split into four distinct signals at 3200, 3650, 4200 and 4850 ppm [13]. These signals have been assigned to the existence of four distinct oxidation states for V atoms in the unit $(VO)_2P_2O_7$ cell at 4.44+, 4.19+, 3.79+ and 3.69+, respectively, in accordance with previous calculations of the individual bond strengths [14]. We used these results to measure the oxidation states of the V atoms in the unit cell of $(VO)_2P_2O_7$ for the VPCo4-Ia and VPCo4-Iaa catalysts and to measure the V(V) contribution from the spectra recorded at room temperature (Table 1): the V(V) contribution is less developed for VPCo4-Iaa as compared to VPCo4-Ia but the $(VO)_2P_2O_7$ unit cell appears slightly more oxidized for VPCo4-Iaa as compared to VPCo4-Ia. This indicates that there is a strong effect of the ligand associated to the dopant in the oxidation state of the Co-VPO promoted

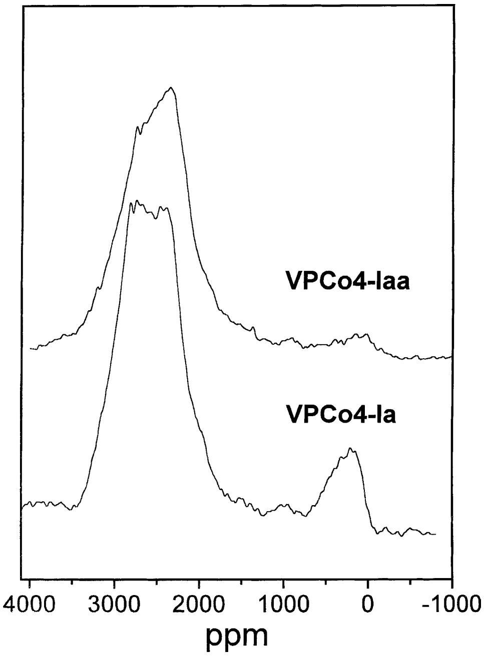

Fig. 3. ^{31}P SEM NMR spectra of promoted catalysts.

Table 1
Contribution of the different V oxidation states (%) calculated from the ^{31}P SEM NMR data on VPOCo4-Ia and VPOCo4-Iaa catalysts

V oxidation state	VPCo4-Ia	VPCo4-Iaa
Four distinct oxidation states for V atoms in the unit $(VO)_2P_2O_7$ cell		
3.69 (3100 ppm)	12.0	10.5
3.79 (2750 ppm)	32.2	33.9
4.19 (2350 ppm)	28.0	25.4
4.44 (2200 ppm)	17.1	25.1
V(V) contribution		
$5-\delta$ (300 ppm)	4.7	0
5 (0 ppm)	6.1	5.1

catalysts: acetate favors V(V) as compared to acetyl acetonate.

The FT-IR spectra of the precursors diluted in fluorolube were obtained trying to detect the presence of other phases besides the vanadyl acid phosphate hemihydrate (Fig. 4). All the spectra show the fingerprints of this phase plus other three bands assigned to the C=C vibration in the plane of aromatic rings (1509, 1492 and 1450 cm^{-1}). They reveal the presence of benzylalcohol and benzaldehyde retained in the dried precursors [9]. In the VPCo4-Ia additional bands at 1564 and 1430 cm^{-1} indicate the presence of the cobalt acetate in the dried solid. Similarly, the absorption bands at 1525 and 1430 cm^{-1} in the VPCo4-Iaa are due to residual acetyl acetonate. In the catalyst refluxed at 393 K (VPCo4-HTI), the signal at 1526 cm^{-1} was not observed. This may be due to the increased interaction between the solid and the salt [12]. As expected all these bands belonging to organic compounds had disappeared in the equilibrated catalysts. All of them exhibit the characteristic signals belonging to vanadyl pyrophosphate. No $VOPO_4$ signal could be detected in any of the spectra. The Raman spectra of the equilibrated catalysts do not show any of the characteristic bands of V(V) phases [12].

We have reported earlier [15] that another key feature in VPO catalysts is the presence of strong Lewis acidity. When acetonitrile was adsorbed at room temperature, three bands are observed in all the catalysts. One, at 2252 cm^{-1}, coincident with that observed for the CN stretching in liquid phase, in the condensed base, which is assigned to physisorbed species. Another at 2297 cm^{-1} corresponding to the Fermi resonance of the CN groups and a third one at higher wavenumber assigned to acetonitrile adsorbed on very

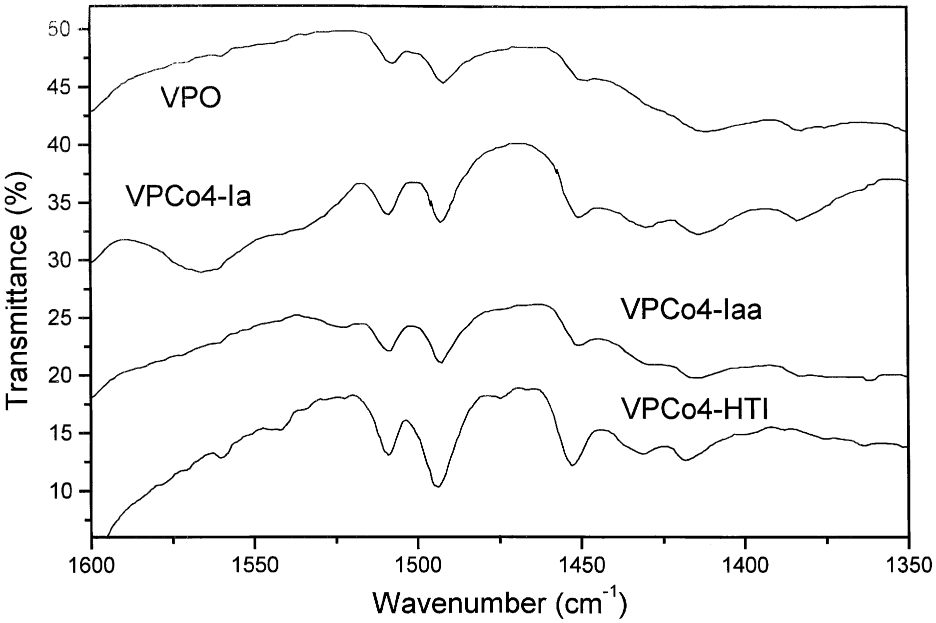

Fig. 4. FT-IR spectra of promoted and unpromoted precursors.

Table 2
Lewis acidity determined by acetonitrile adsorption

Solids	$\Delta\nu$[a] (cm^{-1})		I_{2322}/I_{2297}[b]		Reference
	Very Strong	Medium strong	298 K[c]	423 K[d]	
$AlCl_3$	76	–			[16]
SAPO-5	66	–			[17]
ZnO	–	28			[19]
VPO	74	21			[18]
VPO	68	16	0.56	0.48	This work
VPCo4-Ia	68	–	0.6	1.89	This work
VPCo4-Iaa	68	–	0.69	1.14	This work
VPCo4-HTI	68	16	0.53	1.75	This work

[a] Shift frequency from νCN in the liquid phase (2252 cm^{-1}).
[b] Relative intensity of FT-IR bands at $\nu = 2322$ and 2297 cm^{-1}.
[c] Acetonitrile in the gas phase.
[d] After evacuation at 423 K.

strong Lewis sites. In Table 2, it is reported that this latter band is characteristic when the base is adsorbed in $AlCl_3$ and SAPO-5 [16,17] very strong Lewis acids. In addition, a fourth band was observed at 2270 cm^{-1} in the unpromoted VPO catalyst. This band is assigned to the interaction of the base with medium strong Lewis acid sites [18]. A similar displacement of this band was reported for the adsorption on ZnO [19] (Table 2). After evacuation at 423 K, the band at 2252 cm^{-1} disappears from all the solids, while the bands at 2322 cm^{-1} are still there. The intensity ratio between the bands at 2322 and 2297 cm^{-1} has been taken as an indication of the concentration of very strong Lewis acid sites. This ratio is shown in Table 2. Note the significant increase in this ratio after promoter addition. Furthermore, this ratio is affected by both the type of impregnating salt used and the method of impregnation. In the discussion we will come back to this point in connection with the catalytic behavior.

The oxidation state of vanadium on the surface of VPO catalysts has been a highly controversial matter for the last few years. The results obtained through curve fitting of the spectra in the O 1s–V 2p region are shown in Fig. 5 for VPCo4-Ia and VPCo4-Iaa catalysts. In all the cases studied, the curve fitting leads to a single, well-defined binding energy for V $2p_{3/2}$. The peak was centered at 517.7 ± 0.1 eV with FWHM of 2.3 eV. Binding energies were referred to the O 1s line at 532.2 eV.

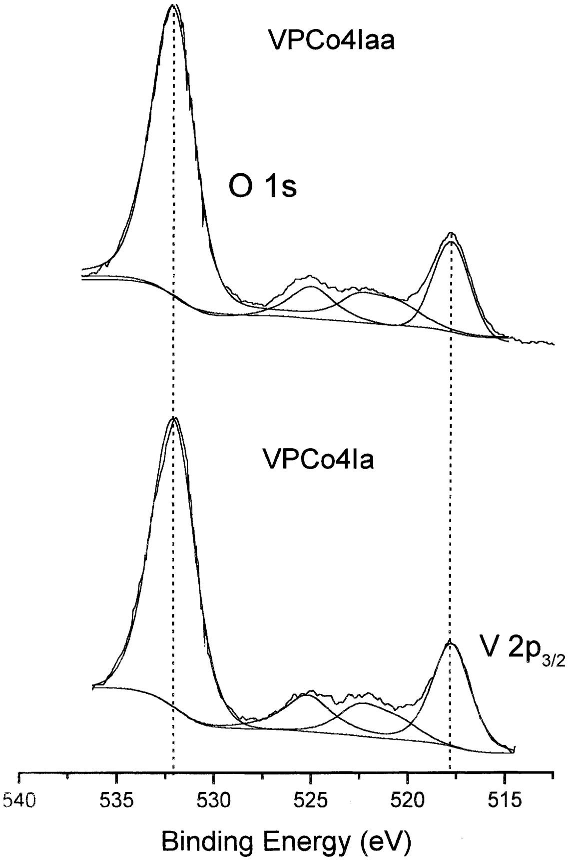

Fig. 5. XPS spectra of the O 1s–V 2p region.

To avoid the use of a reference, an additional method was used to find out the vanadium oxidation state. This method is based on the difference in the BEs of the O 1s and V $2p_{3/2}$ signals (Δ[O 1s–V $2p_{3/2}$]). Table 3 shows that all the equilibrated catalysts give Δ values of 14.4±0.1 eV. The average vanadium oxidation state was calculated using the Δ value correlation proposed by Coulston et al. [20]. These calculated values are all around 4, suggesting that only V(IV) is present on the surface of the equilibrated catalysts.

The binding energies of reference compounds and equilibrated catalysts are summarized in Table 3. The Co $2p_{3/2}$ BE is 780.5 eV for CoO. For Co promoted vanadyl pyrophosphate the binding energy is much higher. For the VPCo4-Iaa and VPCo4-Ia catalysts, the Co $2p_{3/2}$ binding energies (Table 3) were different. The value of 783.3 eV indicates that the presence

Table 3
The surface vanadium oxidation states and binding energies for cobalt in the equilibrated catalysts

Solids	Δ[O 1s–V $2p_{3/2}$] (eV)	V_{ox}[a]	Co $2p_{3/2}$ (eV)	Satellite (eV)	I_{Sat}/IMP
VPO	14.3	4.09			
VPCo4-Ia	14.3	4.09	782.7 (3.0)	787.4 (7.3)	1.4
VPCo4-Iaa	14.5	3.96	783.2 (3.3)	787.4 (5.4)	0.8
VPCo4-HTI	14.3	4.09	783.3 (3.3)	788.0 (5.0)	0.7
CoO			780.5	786.9	0.9
Co_3O_4			779.5	788	–
$Co(OH)_2$			781.0	786.4	–

[a] Using the following correlation: $V_{ox} = 13.82 - 0.68(\Delta[\text{O 1s–V } 2p_{3/2}])$, from [16].

of CoO on the surface is unlikely. On examining the XPS profile of the impregnated catalysts, the Co 2p spectrum has an intense shoulder at ∼788 eV. The Co 2p satellite intensities approach satellite/main peak intensity ratios observed for bulk CoO, while the strong satellite lines are centered about 4.7–4.2 eV above the principal line. The $2p_{1/2}$–$2p_{3/2}$ spin–orbit splitting is 15.7 eV for the three catalysts.

We have previously reported [12] the surface atomic ratios for these equilibrated catalysts. A high surface P/V ratio (P/V ≈ 2.6) was observed while all the catalysts have similar Co/V surface ratios equal to 0.28 ± 0.02.

4. Discussion

The addition of cobalt affects the catalytic performance of VPO formulations. As reported in a previous contribution of our group [8], the optimum behavior of VPO is observed at an intermediate cobalt loading using cobalt acetyl acetonate to impregnate the parent $VOHPO_4 \cdot 0.5H_2O$ precursor (Fig. 1).

The question is how the Co addition affects properties such as Lewis acidity, the co-existence of $VOPO_4$ phases, and/or the presence of highly dispersed V(V) centers within the $(VO)_2P_2O_7$ structure. The latter two matters were investigated both at the bulk and surface level. And finally, is Co in the equilibrated catalyst in the form of cobalt oxides, phosphates or as highly dispersed species?

The key role played by Lewis acidity in the oxidation of *n*-butane to maleic anhydride has been recognized for a long time [21]. They would be directly involved in the activation of the alkane. The Lewis sites are pictured as the coordinatively unsaturated (CUS) V(IV) cations exposed on the [1 0 0] plane. According to Abon and Volta [22] they could be either easily oxidized or hydroxylated.

Wachs et al. [23] studying model catalysts, reported that the presence of acidic metal oxide sites adjacent to the surface vanadia species has a beneficial effect upon the oxidation of *n*-butane. Furthermore, they found a correlation between maleic anhydride selectivity and the Lewis acid strength of the metallic promoters. In brief, they concluded that the oxidation of *n*-butane to maleic anhydride is a function of both the redox properties and the acidic character of the catalyst. Guliants et al. [24] also concluded that the promoters play an important role in the control of the surface acidity of VPO formulations. More specifically, in the case of Co addition Zazhigalov et al. [7] said that this metal enhances the acidity of the VPO solids, increasing the selectivity to maleic anhydride.

Our data show that the addition of cobalt increases the number of Lewis centers but does not affect their strength (Table 2). The concentration of very strong Lewis sites is the highest for the VPO solid impregnated with Co acetate. Table 4 shows that for GHSV ranging between 900 and 2500 h^{-1} and different conversions (50, 65 and 80%) there is an optimum concentration of very strong Lewis acid sites for which the maximum selectivities are achieved. The solid impregnated under reflux exhibits an enhanced concentration of acid sites compared to the VPCo4-Iaa. The former formulation turns out to be less selective than the latter. The highest concentration of acid sites was observed in the solid impregnated with cobalt acetate. This formulation shows low selectivities similar to those observed with unpromoted VPO (Table 4). A maximum in the selectivity versus concentration of acid sites was also reported by Zazhigalov et al. [25]

Table 4
Acidity measurement, NMR and catalytic data of equilibrated catalysts

Catalysts	V(IV)/V(V)[a]	V(V) phases (XRD)	I_{2322}/I_{2297}[b] (423 K)	GHSV = 900 h^{-1}		GHSV = 2500 h^{-1}	
				S $(x = 60)$[c]	S $(x = 80)$[c]	S $(x = 65)$[c]	S $(x = 80)$[c]
VPO	–	No	0.48	45	32	41	35
VPCo4-Iaa	18.6	No	1.14	60	59	61	61
VPCo4-HTI	–	No	1.75	50	53	49	50
VPCo4-Ia	8.3	Yes	1.89	39	35	40	42

[a] Determined from NMR measurements.
[b] Relative intensity of FT-IR bands. This ratio gives an estimate of the very strong Lewis acid site concentration.
[c] Maleic anhydride selectivities measured at conversion values given between brackets.

for several promoters added in varying proportion to the VPO solid. The existence of such a maximum might be interpreted as a trade-off between the retention of the anhydride and the early desorption of acidic intermediates. In the case of lower acid site concentration, the product is retained on the surface and burnt while at the other end, the highest acid site concentration produces an early desorption of intermediates which are easily oxidized to CO_x and H_2O.

Going now to the role played by the presence of tiny amounts of V(V) phases, let us briefly review the latest conclusions reached in the literature about this matter. Trifirò [26] reported that no V(V) phases could be detected in industrial equilibrated catalysts. In model organic catalysts, Guliants et al. [27] reported that the most selective ones contained no minor $VOPO_4$ phases. They sustained that their experimental data did not support the model of *n*-butane oxidation on microcrystalline domains of V(V) orthophosphates in VPO catalysts. Their ^{31}P spin echo NMR spectrum also showed the presence of only vanadyl pyrophosphate in the equilibrated catalyst.

López Granados et al. [28] reported a high stability against oxidation (confirmed by XPS) of V(IV) in well-crystallized unpromoted vanadyl pyrophosphate, the sole phase present in the equilibrated catalysts. This stability could explain the better catalytic properties of this phase: V(IV) sites prevail over the V(V) centers. Their TPD results suggest that V(IV) is capable of anchoring and activating the hydrocarbons and that V(IV) transforms and releases the HCOs (partially dehydrogenated and oxidized hydrocarbons) formed after activation of hydrocarbons at lower temperatures than V(V), favoring more selective transformations.

Only in one case (Table 4) did we find a tiny signal at $2\theta = 18.1^\circ$ which is likely to belong to $VOPO_4$. It should be noted, however, that this signal was not seen when the XRD pattern of this catalyst was obtained within a few days after the end of the run [9]. All the other catalysts do not show the presence of $VOPO_4$ phases either by XRD or by ^{31}P NMR.

Several authors have also claimed that the V(V) species are associated with the creation of structural defects. In our case, we found that ^{31}P NMR clearly indicates the presence of a small concentration of isolated V(V) species inserted in the $(VO)_2P_2O_7$ structure in the case of the most selective catalyst (Fig. 3 and Table 4).

Now, let us discuss our results in terms of the current literature concerning the state of Co on the surface and the presence of V(V) on the surface.

On examining the XPS profile of the impregnated catalysts, the Co 2p satellite intensities approach satellite/main peak intensity ratios observed for bulk CoO, while the strong satellite lines are centered about 4.2–4.7 eV above the principal line. Besides, $2p_{1/2}$–$2p_{3/2}$ = 15.7 eV. These observations indicate that Co(II) is not being oxidized to Co(III).

The high BEs (783.3–782.7 eV) might be related to strong interaction between cobalt and other atoms of the solid matrix and/or to highly dispersed cobalt. Binding energies of 783 eV were reported [29] for the ion exchanged form of cobalt in zeolites. In these solids, the higher than normal binding energy is suggestive of cobalt in a highly oxidizing environment. Zazhigalov et al. [7] reported a similarly high binding energy of 783.0 eV for Co-promoted VPO catalysts. They sustained that this high binding energy can be considered as an additional indication of the formation of cobalt phosphate (detected by XRD). On the other hand, they suggested the existence of strong interactions between cobalt atoms and phosphate groups with a shift of bonding electrons towards the phosphate anions.

In our catalysts, the Co/V nominal ratio is lower than 0.13, and no cobalt phosphates were detected by XRD, FT-IR and Raman spectroscopies. Qualitatively considering the high P/V surface ratio and the fact that all the catalysts have similar Co/V surface ratios, it is possible that the high BE of Co $2p_{3/2}$ be symptomatic of the presence of surface cobalt pyrophosphate. This surface compound does not have long-range, three-dimensional order because characteristic XRD lines have not been observed. However, binding energies are not a sufficient criterion to confirm the presence of a given compound.

A difference in BE was observed between the two impregnated catalysts, and could be related to different surface Co(II) interactions or to a change of the cation distribution at the surface. Two different impregnating salts (cobalt acetate and acetyl acetonate) might produce catalysts with varying strength in the Co–pyrophosphate interaction or different Co dispersion. However, no differences were observed between the catalysts prepared with the same impregnation salt and different impregnation method.

In a previous XPS study [30], it was concluded that the excess phosphorus not only prevents the oxidation of the bulk to more stable V(V) phases, but also it limits the total oxidation of the surface under severe conditions. Besides, the authors have checked their ability to detect surface V(V) by XPS in Co-impregnated catalysts [9]. Through in situ oxygen treatments, they have found that V(V) proportions higher than 10% can be detected on the surface. The XPS results shown here indicate that only V(IV) centers are present on the surface. Note, however, that the catalysts were always analyzed ex situ.

Trifirò and coworkers [1] propose that the defects in the crystalline structure of the vanadyl pyrophosphate create strain in the V–O–P bonds leading to the generation of very strong Lewis sites. In our catalysts, the polarization of the V–O–P bonds could be induced by the presence of Co(II). Besides, a similar effect due to the presence of isolated V(V) in the bulk of equilibrated catalysts cannot be discarded.

5. Conclusions

The beneficial effect of cobalt upon the performance of the VPO formulations is related to the following:

- The increased concentration of very strong Lewis acid sites. However, beyond a certain limit, the excessive abundance of these surface sites decreases the selectivity of the system (Table 4).
- The appearance of a small concentration of isolated V(V) centers which were detected in the most selective catalyst prepared using the acetyl acetonate ligand rather than the acetate one (Fig. 3). Note, however, that when V(V) phases were detected (NMR and XRD) the selectivity went down (Table 4).
- The presence of cobalt phosphate suggested by the XPS data may help stabilize the excess phosphorus present in these and commercial formulations. This is in agreement with the findings of Zazhigalov et al. [7].

Acknowledgements

The authors wish to acknowledge the financial support received from UNL (CAI+D 96 Program). They are also grateful to the Japan International Cooperation Agency (JICA) for the donation of the major instruments used in this study. Thanks are finally given to Prof. Elsa Grimaldi for editing the English paper.

References

[1] G. Centi, F. Trifirò, J. Ebner, V. Franchetti, Chem. Rev. 88 (1988) 55.
[2] F. Ben Abdelouahab, R. Olier, M. Ziyad, J.C. Volta, J. Catal. 134 (1992) 151.
[3] G. Hutchings, Appl. Catal. 72 (1991) 1.
[4] G. Hutchings, R. Higgins, J. Catal. 162 (1996) 153.
[5] Y. Takita, K. Tanaka, S. Ichimaru, Y. Mizihara, Y. Abe, Y. Ishihara, Appl. Catal. A 103 (1993) 281.
[6] G. Hutchings, C. Kelly, M.T. Sananés-Schulz, A. Burrows, J.C. Volta, Catal. Today 40 (1998) 273.
[7] V.A. Zazhigalov, J. Haber, J. Stoch, A. Pyatnitzkaya, G.A. Komashko, V.M. Belousov, Appl. Catal. A 96 (1993) 135.
[8] L. Cornaglia, C. Carrara, J. Petunchi, E. Lombardo, Appl. Catal. A 183 (1999) 177.
[9] L. Cornaglia, C. Carrara, J. Petunchi, E. Lombardo, Catal. Today 57 (2000) 313.

[10] S. Sajip, J.K. Bartley, A. Burrows, M.T. Sananes-Schulz, A. Tuel, J.C. Volta, C.J. Kiely, G.J. Hutchings, New J. Chem. 25 (2001) 125.

[11] M.T. Sananes-Schulz, F.B. Abdelouhab, G.J. Hutchings, J.C. Volta, J. Catal. 163 (1996) 346.

[12] C. Carrara, S. Irusta, E. Lombardo, L. Cornaglia, Appl. Catal. A: Gen. 217 (2001) 275.

[13] A. Tuel, L. Cannesson, J.C. Volta, Coll. Surf., Phys. Ing. Aspects 158 (1999) 97.

[14] I.D. Brown, K.K. Wu, Acta Cryst. B 32 (1976) 1957.

[15] L. Cornaglia, E. Lombardo, J. Anderson, J.L. García Fierro, Appl. Catal. A 100 (1993) 37.

[16] K.F. Pursell, R.S. Drago, J. Am. Chem. Soc. 88 (1966) 919.

[17] L.M. Kustov, S.A. Zubkov, A.Y. Khodakov, V.B. Kazanskii, Kinet. Catal. 33 (1992) 169.

[18] G. Busca, G. Centi, F. Trifirò, V. Lorenzelli, J. Phys. Chem. 90 (1986) 1337.

[19] J.C. Lavalley, C. Gain, C. Paris, C.R. Acad. Sci. Ser. C 228 (1979) 177.

[20] G.W. Coulston, E.A. Thompson, N. Herron, J. Catal. 163 (1996) 122.

[21] G. Centi, G. Golinelli, G. Busca, J. Phys. Chem. 94 (1990) 6813.

[22] M. Abon, J.C. Volta, Appl. Catal. A: Gen. 157 (1997) 173.

[23] I.E. Wachs, J.M. Jeheng, G. Deo, B.M. Weckhuysen, V.V. Guliants, J.B. Benziger, S. Sundaresan, J. Catal. 170 (1997) 75.

[24] V. Guliants, J. Benziger, S. Sundaresan, I. Wachs, A. Hirte, Catal. Lett. 62 (1999) 87.

[25] V. Zazhigalov, J. Haber, J. Stoch, I. Bacherikova, G. Komasko, A. Pyatnitskaya, Appl. Catal. 134 (1996) 225.

[26] F. Trifirò, Catal. Today 41 (1998) 21.

[27] V.V. Guliants, J.B. Benziger, S. Sundaresan, I.E. Wachs, J.-M. Jehng, J.E. Roberts, Catal. Today 28 (1996) 275.

[28] M. López Granados, J.L. García Fierro, F. Cavani, A. Colombo, F. Giuntoli, F. Trifirò, Catal. Today 40 (1998) 251.

[29] J. Stencel, V. Rao, J. Diehl, K. Rhee, A. Dhere, R. De Angelis, J. Catal. 84 (1983) 109.

[30] L. Cornaglia, E.A. Lombardo, Appl. Catal. A 127 (1995) 125.